

## COMPARATIVE ANALYSIS OF SILICON CARBIDE WITH ZIRCONIUM-BASED ALLOYS

**R Daniel de Souza Gomes<sup>1</sup> and Claudia Giovedi<sup>2</sup>**

<sup>2</sup> Instituto de Pesquisas Energéticas e Nucleares (IPEN / CNEN - SP)  
Av. Professor Lineu Prestes 2242  
05508-000 São Paulo, SP  
[dsgomes@ipen.br](mailto:dsgomes@ipen.br)

<sup>2</sup> LabRisco – Universidade de São Paulo  
Av. Prof. Mello Moraes 2231  
05508-030 São Paulo, SP, Brazil  
[claudia.giovedi@labrisco.usp](mailto:claudia.giovedi@labrisco.usp)

### ABSTRACT

According to international plans, the nuclear reactor fleet should reduce operational risk and avoid severe accidents. Around the world, there are 450 nuclear power reactors in operation, which supply about 11% of the electricity consumed. There are programs, such as Advanced Fuels Campaign (AFC), that plan to develop a more tolerant fuel system by 2025. These plans follow security concepts that present two options capable of replacing zirconium alloys used as cladding. The better candidates are metallic alloys and ceramic materials. Until the mid-1970s, austenitic steel was the main coating option. Recently, iron-based alloys have become short-term solutions composed of iron-chromium-aluminum (FeCrAl) alloys. However, there are various advantages from using multilayer of silicon carbide (SiC) and ceramic composites. Silicon carbide has higher corrosion resistance, coupled with higher mechanical strength compared to zirconium alloys. Upon steam contact, ceramic cladding mitigates hydrogen buildup, avoiding explosion risk. This study presents a comparison of the thermal and mechanical properties between zirconium alloys and ceramic alternatives. Ceramic materials show desirable mechanical strength, such as high initial crack resistance, stiffness, ultimate strength, impact response, and high corrosion resistance. SiC has a lower neutron cross-section with significant safety margins.

### 1. INTRODUCTION

Nuclear fuel cladding has several functions to ensure a nuclear reactor operates safely. The cladding is the first barrier that prevents the release of radioactive isotopes and should contain fission products and gases under both service and accident situations. The coating also ensures proper heat transfer of the fuel to the coolant to maintain safe operating conditions. Zirconium alloys were the first cladding material used in civilian reactors, by Admiral Rickover in the Shippingport Atomic Power Station in 1957. Zirconium-based alloys (zircalloys) exhibit a low thermal neutron absorption cross-section, superior corrosion resistance, and excellent dimensional stability in an irradiation environment [1]. In the mid-1970s, zircalloys replaced stainless steels (SS) as the desired cladding material. Stainless steel is in a class of ferritic alloys that contain a minimum of 10.5% chromium, also has easy manufacture. Austenitic steels are highly workable, have adequate strength, and exhibit excellent corrosion resistance, but have a high neutron cross-section [2].

Zirconium alloys exhibit low neutron cross-section and acceptable corrosion performance under service temperatures of around 300° C. However, zircalloys have several drawbacks, such as cladding embrittlement, undesirable exothermal oxidation above 1204° C, and the oxidation reaction becoming autocatalytic, consequentially can release an enormous amount of hydrogen followed by an explosion [3].

Since 1989, global nuclear agencies showed a significant worry with the danger of explosion of hydrogen produced corrosion of zirconium alloys due to the three-mile island accident. The turning point in nuclear fuel cladding technology was an accident that occurred at the Fukushima Daiichi Nuclear Power Plant in Japan in 2011. Globally, the accident influenced a negative public opinion on nuclear safety procedures. The years following the Fukushima accident have seen a significant rise in dedicated efforts to improve tolerance of fuel to severe accident scenarios. The US Department of Energy (DOE) has started a comprehensive research and development program, following the US Advanced Fuel Campaign and Fuel Cycle Development (AFC), in charge of identifying fuel-coating systems that have a higher tolerance to accident scenarios, to develop them for viable use [4].

## **1.1 Metallic and Ceramic Options to Replace Zirconium Alloys**

Initially, US-DOE sponsored Accident Tolerant Fuel (ATF) plans were to become a global collaborative work. Universities and fuel suppliers tried to develop advanced materials to replace the zirconium-based alloys for light water reactors (LWRs). The metallic alternative under consideration was iron-chromium-aluminum (FeCrAl) alloys [5]. Ceramic materials, such as silicon carbide (SiC), FeCrAl, and SiC, exhibit superior corrosion characteristics and much slower oxidation kinetics in high-temperature steam when compared to zircalloys. Advanced cladding materials should provide larger safety margins for transient conditions, permit long cycle length, increase burn-up discharge, and uprate power proposed to nuclear units in operation [6].

The Acheson process discovered in 1891 was the first preparation of silicon carbide as results from synthesizing graphite and silica, or sand [7]. Today, SiC has many applications for a wide range of industries. SiC has good acceptance on nuclear industry adopted SiC because it proved to be a good alternative which exhibited an excellent thermal conductivity, low thermal expansion, and exceptional corrosion resistance. There are many options for using silicon carbide for nuclear cladding. One option is using SiC in different ceramic matrix composites (CMC) produced with silicon carbide (SiC) matrices and SiC, or carbon fibers. CMC fiber comprises a high-strength silicon carbide fiber with a reinforcement phase in high-temperatures. The chemical method used to produce carbide composites may include chemical vapor infiltration (CVI), or chemical vapor deposition (CVD) [8].

The better architecture proposed to SiC as cladding shows three layers, the inner and outermost layers which include monolithic SiC, while the middle layer is of a SiC fiber-wound composite. Silicon carbide showed excellent irradiation tolerance, also adequate chemical compatibility with uranium dioxide (UO<sub>2</sub>) [9]. In the triplex configuration, the SiC inner layer has an essential function which is preventing radioactive fission products release to leave the fuel and diffusing into the coolant. The SiC triplex tubes consisting of a SiC inner layer, a SiC/SiC intermediate layer, and a SiC-CVD as an outer layer. The composite fibers used in the middle layer must provide better fracture toughness and increased hoop strength [10].

However, a simple tube of FeCrAl formed by a single layer is also a cladding contender. Advanced fuel projects have researched aluminum-bearing ferritic steels, such as Kanthal-APMT and several types of FeCrAl alloys as a cladding material. FeCrAl comprises iron alloys, which can contain 10 to 22 wt % Cr and 3 to 6 wt % dissolved Al. Another conceptual cladding includes multiple components, also known as coated cladding, which utilized a thin layer of chromium sprays deposited over zircalloys. This concept cladding displayed a modification of current Zr-based alloys coupled with different protective layers and dopants.

Existing configurations using bilayers coating based on  $\text{ZrO}_2$  and FeCrAl, that showed conceptual responses. Ferritic alloys composed of several materials showing vast gamma resistance routed via complex metallurgical processes. These effects produced by several chemical additions, such as Mo, Nb, Ti, and C. Today, there is a consensus in the nuclear community that ferritic alloys exhibit a wide variety of compositions which can feasibly replace zircalloys [11]. In this investigation, the focus is on an oxide dispersion strengthened (ODS) alloy, known as Kanthal Advanced Powder Metallurgical (APMT) alloy. Kanthal-APMT met the requirements to manufacture cladding tubes with a length of 4 m, working pressure on 0.9 MPa, and temperatures that can reach 1000 °C. Many ferritic oxide dispersions strengthened steels are being tested today, such as PM2000.

## **1.2 Fuel Performance Codes**

In this study, the simulation contains physical material properties of Kanthal-APMT, also features of monolithic SiC and one intermediate layer of CMC. Fuel codes are tools capable of predicting fuel performance under irradiation. These systems can estimate the effects produced by power variations and boundary conditions under quasi-steady-state conditions. The systems can also include many situations, such as long periods at constant power or moderate power ramps. Licensing codes showed that acceptable results must predict all output parameters. There are several safety limits defined empirically, including maximum fuel temperature, deformation, swelling, and fission gas release (FGR). The US Nuclear Regulatory Commission uses to licensing process the fuel codes to audit nuclear power plants (NPPs). One steady-state system can analyze the thermal-mechanical behavior of oxide fuel rods, known as the Fuel Rod Analysis Program Conservative (FRAPCON) [12]. Both fuel codes adopted the models defined in the Materials Property Library (MATPRO), also used in the development of thermal-hydraulic systems [13].

## **2. MATERIALS AND METHODS**

### **2.1 Physical Properties Review**

The materials researched in the ATF and AFC programs went through several phases, including at least two FeCrAl alloy generations. Two alloys, PM2000 and MA956, stood out from alternate formulations [14-15]. There are other alloys developed by Oak Ridge National Laboratory (ORNL), where developed C26M (12%-Cr) and B136Y (13%-Cr), which have more irradiation resistance than Kanthal-APMT. In the second phase, ODS alloys, such as Kanthal-APMT, became preferred when containing 21%-Cr and a fraction of 5%-Al, which proved capable of producing a protective layer.

The SiC triplex configuration would have differences between the monolithic and inner layer of fibers, which allows for higher elasticity [16]. The multilayer configuration should keep several mechanical properties at higher temperatures and remain as a long-term solution compared with Kanthal-APMT. Cladding manufactured based on Triplex SiC has a potentially long-range development timeline. SiC could offer improvements in safety requirements compared with zirconium-alloy. Table 1 shows the compositions of the first generation of FeCrAl tested for AFC programs. Table 2 shows the structure of iron-chromium-aluminum alloys MA956 and PM2000. [16-17]

**Table 1: Zirconium based alloys chemical composition in (%)**

Zr- alloys	Zr	Fe	Cr	Sn	Ni
Zircaloy-4	97.56-98.27	0.28 - 0.37	0.07 - 0.13	1.2 - 1.7	-
Zircaloy-2	98.5	0.07-0.20	0.05 -0.15	1.2 - 1.8	0.03 -0.08
Zirlo	-	0.11	-	0.0-0.99	-

**Table 2: Chemical composition of MA956 and PM2000 alloys**

Chemical Composition	Cr	Al	Ti	Y <sub>2</sub> O <sub>3</sub>	C	Fe
MA-956 (%)	20.0	4.40	0.30	0.50	0.04	Balanced.
PM-2000 (%)	20.0	5.50	0.50	0.50	0.01	Balanced.

Kanthal-APMT is a commercial alloy fabricated by several suppliers, and the Sandvik informed compositions of 68.85%-Fe, 22%-Cr, 5%-Al, with small additions of 0.4%-Mn, 3%-Mo, and 0.7%-Si. APMT shows an elasticity modulus of 220 GPa at room temperature. In temperature ranges of 20° C to 1000 °C, FeCrAls have Young's modulus changing from 220 GPa to 120 GPa, which is higher compared to Zircaloys that exhibiting Young's modulus between 81 GPa and 75 GPa in the same temperature range. Consequentially, FeCrAl alloys are less susceptible to deformation than zirconium alloys. Table 3 summarized the physical properties of advanced materials, where showed higher ultimate tensile strengthen of FeCrAl, also the coefficient of thermal expansion at room temperature [18-23]

**Table 3: Physical properties of advanced materials capable of replacing zircaloys.**

Cladding Material	FeCrAl PM-2000	FeCrAl MA-956	Kanthal APMT	Zr-4	SiC CVD	Tyranno fiber
Density (g/cm <sup>3</sup> )	7.18	7.25	7.25	6.56	3.21	3.1
UTS (MPa)	720	650	740	413	372	2800
Elongation at break (%)	14	9	26	20	-	0.70%
Modulus of elasticity (GPa)	160	172	220	99.3	420	380
CTE, linear (µm/m-°C)	10.7	11.3	12.4	6	4.5	4.5
Heat capacity (kJ/kg-°C)	480	469	480	285	660	669
Melting point	1483	1355	1500	1850	2700	2700
Conductivity (W/m-°C)	10.9	10.9	11	21.5	220	64.6

In the temperature range of 50 °C to 1200 °C, the thermal conductivity of APMT can vary from 11 W/m-k to 29 W/m-k.

Thermal conductivity of Zircaloy-4 is 15% lower than APMT and exhibits lower heat capacity than APMT [17]. The properties of SiC-CVD are from the supplier, Morgan Advanced Ceramics. Also, there are commercial CVI SiC/SiC composites that are very stable under irradiation, such as Hi-Nicalon type-S (Si, C, O) and Tyranno-SA3 fiber (Si, Ti, Zr-1, C, O). The number of fiber filaments used in Tyranno is 1600, while Nicalon is 500. Tyranno fiber showed a thermal conductivity higher than Nicalon. Tyranno and Nicalon are candidates for usage as fuel cladding in gas-cooled fast reactor systems (GFR).

### 2.1.1. Thermal Conductivity

Metallic alloys, such as stainless steel, have a lower thermal conductivity of 16.2 W/m-k at room temperature, compared with Zr-4 and Zr-2 which have a thermal conductivity of 21.5 W/m-k. Similarly, the conductivity of PM2000 is 10.9 W/m-k, and Kanthal-APMT is 11 W/m-k. In the temperature range of 25 °C to 600 °C, the thermal conductivities Kanthal APMT alloys can vary from 11 W/m-k to 21 W/m-k, while the Zr-4 exhibits values of 19 to 21 W/m-k. The irradiation effects measured as displacement per atom (dpa) using on the range of 1 to 5 dpa, reduce the thermal conductivity of SiC for operations temperatures of PWRs. The phonon scattering effect dominates the heat transfer mechanism of SiC, which rapidly saturates after one dpa of crystal defects. Comparatively, the thermal expansion of zircalloys, FeCrAl alloys, and silicon carbide shows slight variations. Figure 1 illustrates the thermal conductivity of metallic alloys [13], [17], [23].

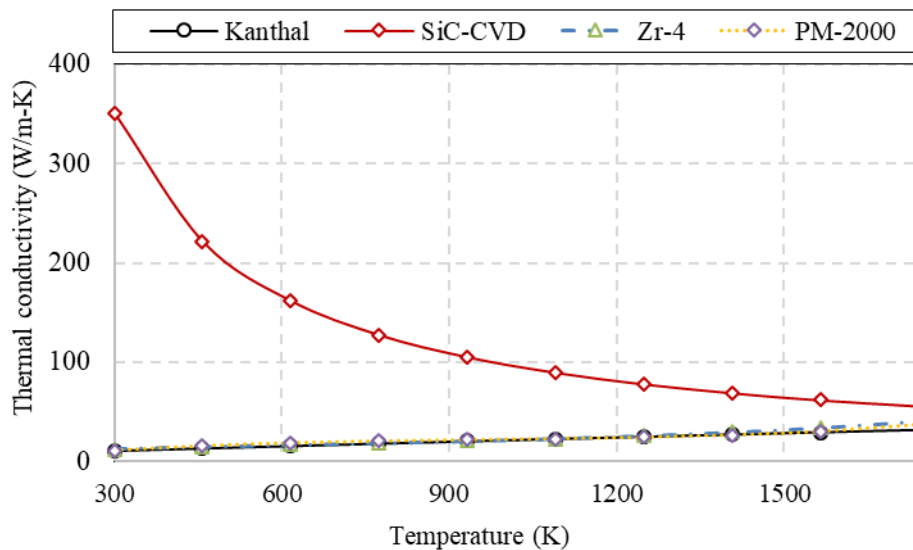


**Figure 1: Thermal conductivity of alloys Kanthal, Zircaloy-4, and PM2000.**

### 2.1.2 Thermal Expansion

Compared with metal alloys, the ceramics have a lower thermal expansion. Comparatively, the zirconium alloys are about three times of silicon carbide. The triplex layer must show lower thermal expansion coefficients, while the zircalloys are  $6.00 \mu\text{m/m}^\circ\text{C}$  and silicon carbide reach  $1.9 \mu\text{m/m}^\circ\text{C}$  at  $25.0^\circ\text{C}$ . Figure 2 illustrates thermal expansion behavior of materials analyzed.

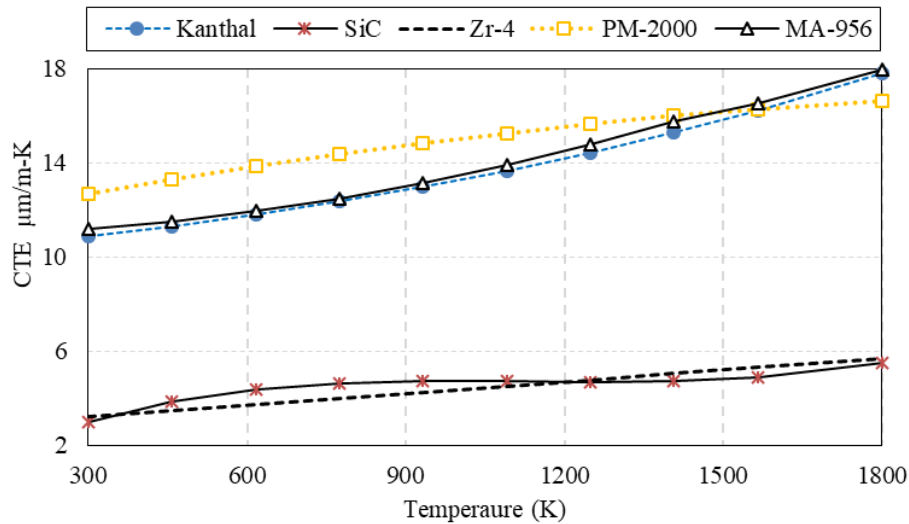


**Figure 2: Thermal expansion of zirconium alloys, FeCrAl alloys, and silicon carbide.**

### 2.1.3 Specific Heat

Ferritic alloys, such as stainless steel, exhibit values of 500 J/kg-K for specific heat, and zirconium alloys have the specific heat in comparison to FeCrAl alloys. Higher heat capacity should improve fuel safety for a slowing of the transient response. For cladding temperatures under steady-state, or normal operation temperature varying around 350 °C, zirconium alloys have a specific heat changing from 306 to 317 J/kg-K, while FeCrAl exhibits values between 574 to 609 J/kg-K in the same temperature conditions. Zirconium alloys have a lower heat capacity than APMT alloys. A high specific heat value can improve fuel safety due to introducing a slower transient response. Figure 3 displays the heat capacities of the materials investigated.

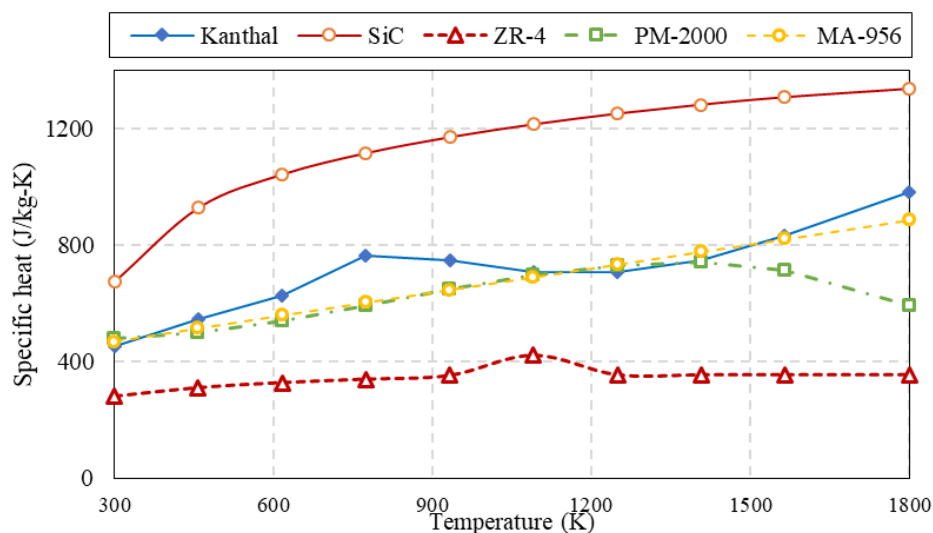


**Figure 3: Heat capacity of zirconium alloys, FeCrAl alloys, and silicon carbide**

## 2.2 Mechanical Properties

Kanthal-APMT features higher elasticity modulus and ultimate yield strength (UTS) of 540 MPa, compared with Zr-4 at 241 MPa and UTS of 740 MPa at room temperature. SiC-CVD has a modulus of elasticity of 420 MPa, a flexural strength of 372 MPa, and a compressive strength of 345 MPa. Thus, the FeCrAl alloy is less susceptible to deformation than zirconium alloys at room temperature. FeCrAl alloys have an elasticity modulus of 151 GPa and Poisson's ratio of 0.3. The FeCrAl alloys, such as MA956, are composed of Fe-20Cr-4.5Al (wt %), and Kanthal APMT have a modulus of elasticity of 160 GPa while zircalloys show a lower value of 99.3 GPa at room temperature. Figure 4 explains the modulus of elasticity of the material considered.

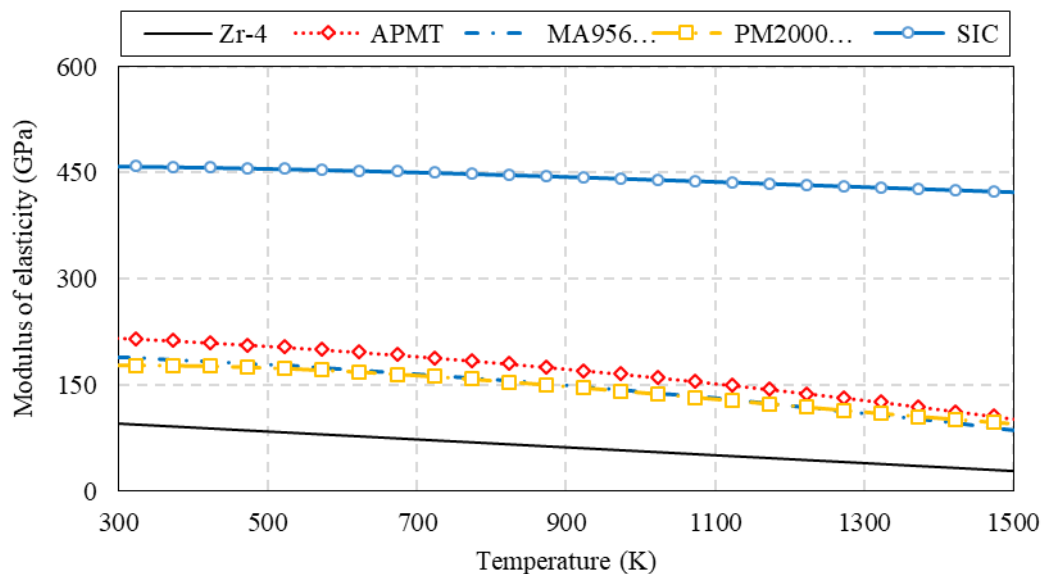


**Figure 4: Modulus of elasticity of zircalloys, FeCrAl alloys, and silicon carbide**

## 3. RESULTS AND DISCUSSION

The simulated reactor is a PWR 17x17, operating with the standard fuel system  $\text{UO}_2/\text{Zr-4}$ . The fuel assembly has 264 fuel rods in a square, 17x17 array. Table 4 summarizes the fuel design parameters used in FRAPCON simulations.

**Table 4: Fuel design parameters of Kanthal APMT and silicon carbide**

Fuel properties	Kanthal	SiC
Cladding outside diameter (mm)	9.50	9.50
Cladding thickness (mm)	0.05715	0.05715
Diametral gap (mm)	0.1651	0.1651
Pellet diameter (mm)	0,81915	0,81915
Pitch (mm)	1,26	1,26
Internal pressure (MPa)	15.51	15.51
Coolant inlet temperature( °C)	279.44	279.44

The cycle length of 1400 days of effective power days (EFPD), reaching 59 MWd/MTU. The number of time steps used is 113, resulting in a power average of 19.22 kW/m. The burn cycle proposed is within safety limits of about 62 MWd/KgU for civilian reactors. Figure 5 exhibits the axial power rate for the average length, localized in the eighth axial node, also in the first and last extreme nodes.

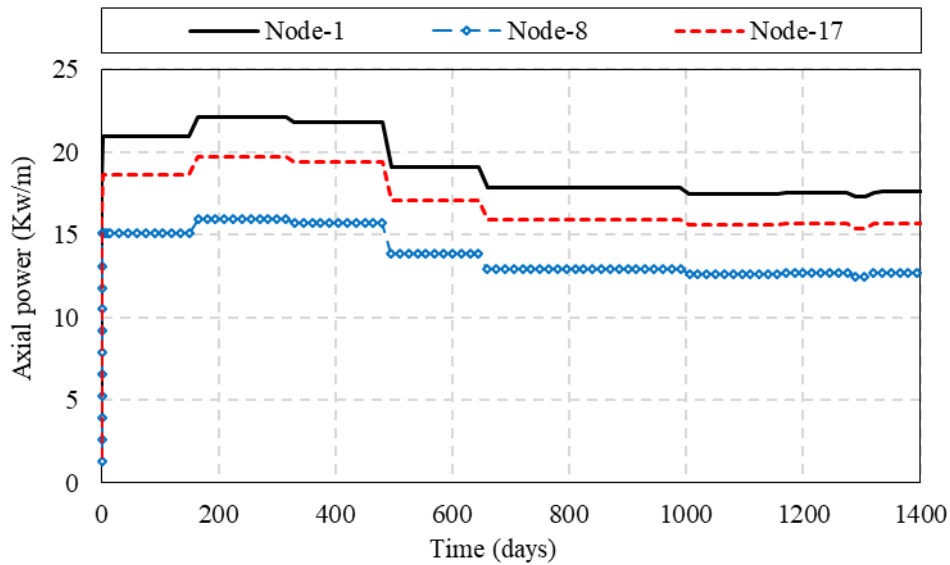


**Figure 5: Axial power on the central node-8 and extreme nodes 1 and 17.**

The fuel temperature shows dependence on a linear power rate. Using Kanthal-APMT, the fuel centerline temperature is higher than Zircaloy-4 because of the reduced thermal conductivity of Kanthal. Therefore, SiC triplex shows better thermal conductivity and exhibits lower temperatures. Figure 6 displays the fuel centerline temperatures of Zr-4, Kanthal-APMT, and SiC Triplex.

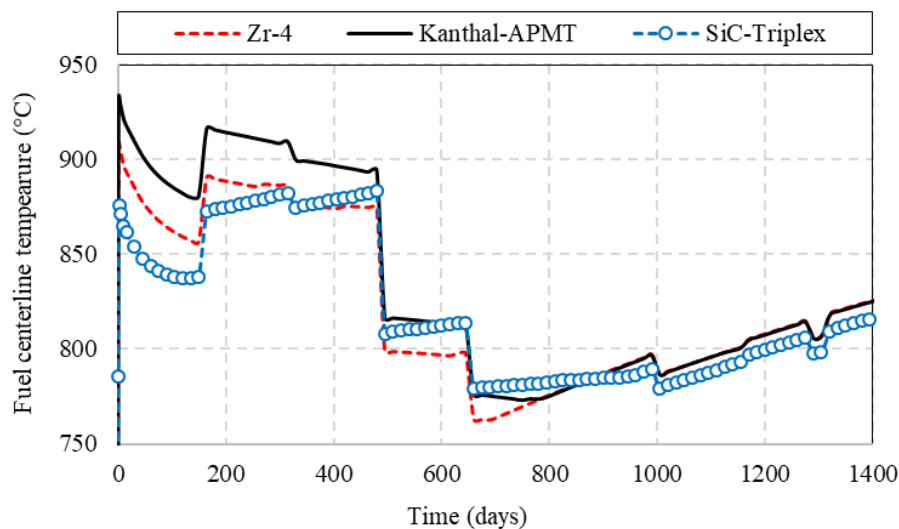


**Figure 6: Fuel centerline temperature for Zr-4, Kanthal-APMT, and SiC-CVD.**



Cladding fracture caused by pellet-cladding interaction (PCI) is an effect that speeds up the gap closure. In addition, the models used to foresee cladding failure have a dependence on crack propagation, based on linear elastic fracture mechanics. The mechanical behavior changed after PCI, which is also a consequence of the stress intensification due to mechanical contact and stress corrosion cracking. Figure 7 shows that gap closure, and PCI begin before Zr-4, then Kanthal is next, with a considerable delay on SiC triplex.

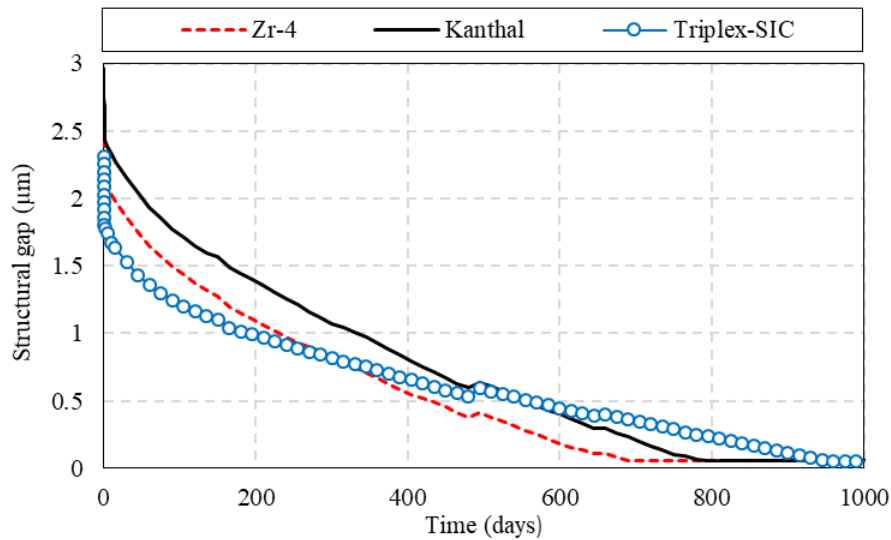


**Figure 7: Structural radial gap closure for Zr-4, Kanthal APMT, and SiC Triplex.**

The axial strain has dependence with the modulus of elasticity and thermal expansion of the material involved. The elastic modulus of Kanthal-APMT is higher than zircaloy, but the thermal expansion coefficient of Kanthal is  $13.1 \mu\text{m/m}$ , and Zr-4 is around  $6 \mu\text{m/m}$  at  $300^\circ\text{C}$ . The SiC Triplex material showed higher thermal conductivity and lowered thermal expansion, producing an enhanced mechanical response. Figure 8 shows the axial cladding strain along the entire length of the fuel rod, 3.65 m divided into 17 axial nodes.

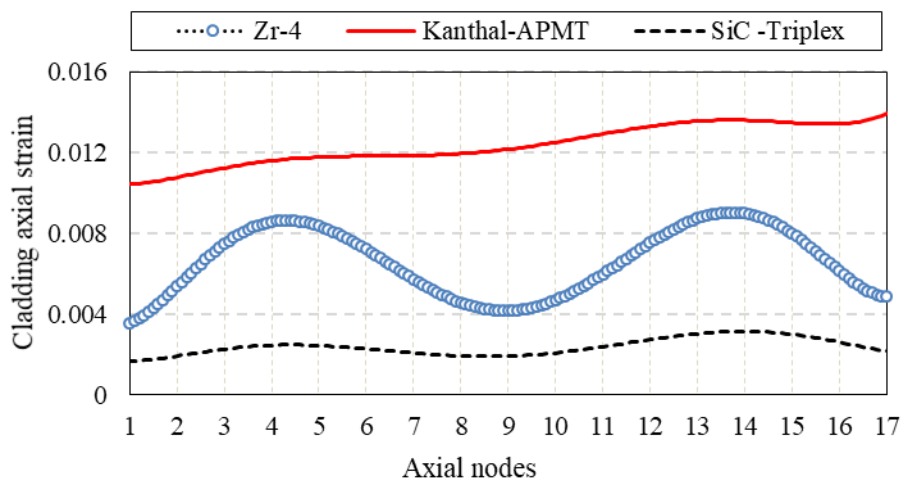


**Figure 8: Cladding axial strain for Zr-4, Kanthal-APMT, and SiC-CVD.**

The hoop strain calculated with FRAPCON follows dependence with the modulus of elasticity and thermal expansion. Also, it verifies that SiC shows a better response due to the higher modulus of the high elasticity, thermal conductivity, and lower thermal expansion.

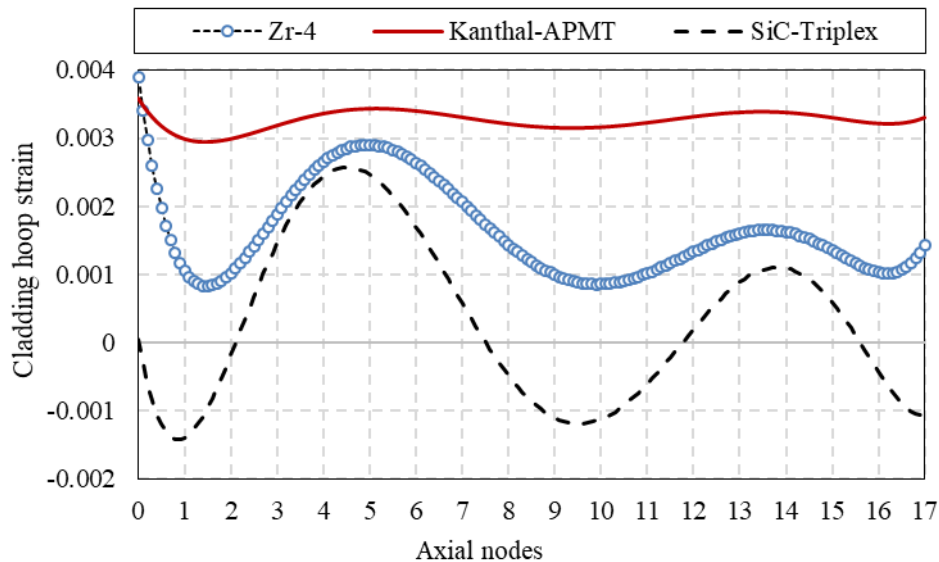


**Figure 9: Cladding hoop strain Zr-4, Kanthal-APMT, and SiC-Triplex**

#### 4. CONCLUSIONS

The comparative investigation performed with FRAPCON fuel code adapted to support FeCrAl alloys and the Triplex layer of SiC appointed that results are acceptable. The behavior of light water reactors during accident scenarios are responsible for a global effort designated to reduce the impact on the civilian's opinion. Early research programs sponsored DOE, and international cooperative work is unanimous in that both advanced materials can avoid hydrogen explosion. However, several considerations must be studied, such as thermal conductivity of SiC under neutron fluence effects. The optimized choice of FeCrAl types such as PM2000, MA956, Kanthal APMT, and other options widely investigated. Also, it may research a thermal cross-section of FeCrAl alloys that promote a substantial loss of energy from fission. Simulation offers a vast horizon of speculations about nuclear requirements planned on the 10 CFR 50.46c, introduced in 2016.

The analysis performed proof that temperature during steady-state operation for both materials suffered reductions. The mechanical behavior also showed that both configurations are better than zircalloys. The gap closure suffers delays if compared with zircalloys. The triplex configuration hugely depends on scattering effects on thermal conductivity that produce different stresses developed in the cladding. The maximum values of tensile stress generated on Triplex and Kanthal can differ by a factor of two under simulation conditions. Besides, there is a strong tendency to replacement zirconium-based alloys on ATF scheduled for 2022. The silicon carbide for three layers needs more effort and shows an expensive and complicated manufacturing route and will consume more investments.

## ACKNOWLEDGMENTS

The authors acknowledged and appreciated the chance offered by the Nuclear and Energy Research Institute IPEN/CNEN/SP–Brazil, and without this technical support, the present investigation could not have been completed.

## REFERENCES

1. P. Bossis, D. Pecheur, K. Hanifi, K., J. Thomazet, M. Blat, "Comparison of the high burn-up corrosion on M5 and low tin Zircaloy-4". In 14th *International Symposium on Zirconium in the Nuclear Industry* **Vol. 3**, pp. 494-525 (2006).
2. C. P. Massey, K. A. Terrani, S. N., Dryepondt, B. A. Pint, (2016). "Cladding burst behavior of Fe-based alloys under LOCA." *Journal of Nuclear Materials*, **Vol. 470**, pp. 128-138 (2016)
3. J. H. Kim, B. K. Choi, J. H. Baek, Y. H. Jeong, "Effects of oxide and hydrogen on the behavior of Zircaloy-4 cladding during the loss of the coolant accident (LOCA)". *Nuclear engineering and design*, **Vol. 236(22)**, pp. 2386-2393 (2006).
4. B. Qiu, Y. Wu, Y. Deng, Y. He, T. Liu, G. H. Su, W. Tian, "A comparative study on preliminary performance evaluation of ATFs under normal and accident conditions with FRAP-ATF code." *Progress in Nuclear Energy*, **Vol. 105**, pp. 51-60 (2018).
5. K. R. Robb, L. J. Ott, M. Howell, *Design and analysis of oxidation tests to inform FeCrAl ATF severe accident models (No. ORNL/SPR-2018/893)*. Oak Ridge National Laboratory. (ORNL), Oak Ridge, Tennessee, United States (2018).
6. K. A. Gamble, T. Barani, D. Pizzocri, J. D. Hales, K. A. Terrani, G. Pastore, "An investigation of FeCrAl cladding behavior under normal operating and loss of coolant conditions." *Journal of Nuclear Materials*, **Vol. 491**, pp. 55-66 (2007).
7. L. L. Snead, T. Nozawa, Y. Katoh, T. S. Byun, S. Kondo, D. A. Petti, "Handbook of SiC properties for fuel performance modeling." *Journal of nuclear materials*, **Vol. 371(1-3)**, 329-377 (2007).
8. C. P. Deck, G. M. Jacobsen, J. Sheeder, O. Gutierrez, J. Zhang, J. Stone, C. A. Back, "Characterization of SiC-SiC composites for accident tolerant fuel cladding." *Journal of Nuclear Materials*, **Vol. 466**, pp. 667-681, (2015).
9. Y. Lee, H. C. No, J. I. Lee, "Design optimization of multi-layer Silicon Carbide cladding for light water reactors." *Nuclear Engineering and Design*, **Vol. 311**, pp. 213-223,(2017).
10. D. Kim, H. G. Lee, J. Y. Park, W. J. Kim, "Fabrication and measurement of hoop strength of SiC triplex tube for nuclear fuel cladding applications." *Journal of Nuclear Materials*, **Vol. 458**, pp. 29-36 (2015).
11. Z. Liu, Y. Li, D. Shi, Y. Guo, M. Li, X. Zhou, S. Du, "Reprint of The development of cladding materials for the accident tolerant fuel system from the Materials Genome Initiative." *Scripta Materialia*, **Vol. 143**, pp. 129-136 (2018).
12. K. J. Geelhood, W. G. Luscher, FRAPCON 4.0: *A Computer Code for the Transient Analysis of Oxide Fuel Rods*. Technical Report No. PNNL-19418, Vol. 1-2, Pacific Northwest National Laboratory (PNNL), Richland, Washington (2015).
13. D. L. Hagrman, G. A. Reymann, *MATPRO-Version 11: A handbook of materials properties for use in the analysis of light water reactor fuel rod behavior* (No. NUREG/CR-0497; TREE-1280). Idaho National Engineering Lab. Idaho Falls (USA) (1979)
14. S. Dryepondt, K. A., Unocic, D. T., Hoelzer, C. P., Massey, B. A. Pint, Development of low-Cr ODS FeCrAl alloys for accident-tolerant fuel cladding. *Journal of Nuclear Materials*, **Vol. 501**, pp. 59-71 (2018)

15. Z. Guoge, R. S. Chandel, "Effect of surface roughness on the diffusion bonding of Incoloy MA 956". *Journal of materials science*, **Vol. 40(7)**, pp. 1793-1796 (2005).
16. C. M. Allison, G. Berna, R. Chambers, E. Coryell, K. Davis, K. D. Hagrman, M. L. McComas, *SCDAP/RELAP5/MOD3. 1 Code Manual Volume IV: MATPRO*. NUREG/CR, 6150, U.S. Nuclear Regulatory Commission, Washington, DC 20555-0001 (1993).
17. D. M. Perez, R. L. Williamson, S. R. Novascone, G. Pastore, J. D. Hales, B. W. Spencer, Assessment of BISON: A nuclear fuel performance analysis code. Idaho National Laboratory, Idaho Falls (2013)
18. E. Rohmer, E. Martin, C. Lorrette, "Mechanical properties of SiC/SiC braided tubes for fuel cladding." *Journal of Nuclear Materials*, **Vol. 453(1-3)**, pp. 16-21 (2014).
19. Y. Yamamoto, M. A. Snead, K.G. Field, K. A. Terrani, Handbook of the Materials Properties of FeCrAl Alloys For Nuclear Power Production Applications (No. ORNL/TM-2017/186). Oak Ridge National Lab. (ORNL), Oak Ridge, TN (United States) (2017).
20. C. Sauder, A. Brusson, J. Lamon, Influence of interface characteristics on the mechanical properties of Hi-Nicalon type-S or Tyranno-SA3 fiber-reinforced SiC/SiC mini composite. *International Journal Of Applied Ceramic Technology*, **Vol. 7(3)**, pp. 291-303 (2010)
21. K.A. Terrani, C. Ang, L. L. Snead, Y. Katoh, "Irradiation stability and thermo-mechanical properties of NITE-SiC irradiated to 10 dpa". *Journal of Nuclear Materials*, **Vol. 499**, pp. 242-247 (2015).
22. Y. Katoh, L. L. Snead, T. Nozawa, S. Kondo, J. t. Busby, Thermophysical and mechanical properties of near-stoichiometric fiber CVI SiC/SiC composites after neutron irradiation at elevated temperatures. *Journal of Nuclear Materials*, **Vol. 403(1-3)**, pp.48-61 (2010).
23. K. G. Field, Handbook on the Material Properties of FeCrAl Alloys for Nuclear Power Production Applications (FY18 Version: Revision 1) (No. ORNL/SPR-2018/905). Oak Ridge National Lab.(ORNL), Oak Ridge, TN (United States) (2018)
24. Y. Lee, H., C., No, J. I. Lee, Design optimization of multi-layer Silicon Carbide cladding for light water reactors. *Nuclear Engineering and Design*, **Vol. 311**, pp. 213-223, (2017)